Green Fabrication of Alginate–Silver Nanocomposite Hydrogel Using Premna serratifolia Leaf Extract: Characterization, Comparative Evaluation, and Enhanced Antimicrobial Efficacy”

P. Naveen[1]

naveen.sklm@gmail.com

Govt.Degree College(A)

Gopi Mamidi[2]

Dr.VSK Govt.Degree College(A)

A. Indira Priyadarsini

Govt.Degree College(A)

Research Article

Keywords: Premna serratifolia, green synthesis, Alginate hydrogel, silver nanocomposite, antimicrobial activity, Biopolymer, Sustained release, Eco-friendly nanotechnology

Posted Date: December 15th, 2025

DOI: https://doi.org/10.21203/rs.3.rs-8189703/v1

Additional Declarations: No competing interests reported.

Abstract

The present study reports the *green fabrication* of a sustainable **alginate–silver nanocomposite hydrogel (Alg–AgNC)** employing the aqueous leaf extract of *Premna serratifolia* L. as a natural reducing and stabilizing agent. The eco-friendly route enables in-situ formation of silver nanoparticles (AgNPs) within a sodium-alginate matrix, eliminating the need for chemical cross-linkers or toxic precursors. The developed nanocomposite was characterized using UV–Vis spectroscopy, FTIR, XRD, SEM, TEM, and zeta-potential analysis. Comparative assessments between biogenic AgNPs and the Alg–AgNC hydrogel evaluated improvements in physicochemical stability, structural integrity, and antimicrobial performance. The Alg–AgNC hydrogel exhibited a surface-plasmon resonance at 428 nm, characteristic Ag (111) reflections in XRD, and uniformly dispersed nanoparticles (20–40 nm) embedded within the alginate network. The zeta potential (–32 mV) and FTIR spectra confirmed enhanced colloidal stability and effective phytochemical capping. Antibacterial testing against *Escherichia coli* and *Staphylococcus aureus* revealed a 1.5–2-fold increase in inhibition-zone diameter compared with free AgNPs, attributed to sustained Ag^{+} release and synergistic polymer–phytochemical interactions. The composite hydrogel remained stable for over 30 days without aggregation, demonstrating mechanical robustness and reusability. This study presents the **first report of an alginate–silver nanocomposite hydrogel synthesized using Premna serratifolia leaf extract**, offering a superior, biocompatible, and sustainable nanomaterial platform for biomedical and environmental applications (1–3, 5, 7–10).

1 Introduction

Nanotechnology has revolutionized biomedical and environmental sciences by enabling the design of materials with exceptional surface reactivity, catalytic efficiency, and bioactivity (1, 2). Among these, **silver nanoparticles (AgNPs)** have drawn major attention for their broad-spectrum antimicrobial efficacy and tunable optical properties (3, 4). However, conventional chemical and physical synthesis routes involve toxic reagents and high-energy processes, often producing unstable colloids that aggregate or oxidize rapidly (1, 2, 4). These concerns have encouraged a global transition toward **green nanotechnology**, wherein plant extracts act as benign bioreductants and stabilizers (3, 5).

1.1 Green synthesis and role of *Premna serratifolia*

Plant-mediated synthesis offers simplicity, sustainability, and low cost. Phytochemicals—particularly phenolics, flavonoids, terpenoids, and lignans—donate electrons to reduce metal ions and cap the nascent nanoparticles (1–3, 5). *Premna serratifolia* L. (Lamiaceae), known as Arani or Headache Tree, is an important Ayurvedic medicinal plant with antioxidant, hepatoprotective, and antimicrobial activities (5, 6). The leaf extract is rich in polyphenols and diterpenoids capable of redox transformations. Although *P. serratifolia* has been used previously for biosynthesis of AgNPs (5) and ZnO NPs (6), **no reports exist on its integration into a polymeric nanocomposite matrix**, presenting an untapped opportunity for multifunctional materials.

1.2 Limitations of standalone nanoparticles

Despite excellent reactivity, free AgNPs face critical limitations:

1. tendency to aggregate, reducing effective surface area;
2. uncontrolled burst release of Ag^+ ions causing cytotoxicity;
3. poor mechanical integrity hindering direct biomedical use; and
4. potential environmental leaching (3, 4, 7).

Hence, current research emphasizes **nanocomposite systems**, where metallic nanoparticles are immobilized within biocompatible polymer matrices to improve stability and functionality (7–10).

1.3 Nanocomposites as next-generation materials

Biopolymer-based nanocomposites mark a paradigm shift from transient colloids to durable, reusable materials. **Sodium alginate**, a polysaccharide from brown algae, is biocompatible, hydrophilic, and forms gels via Ca^{2+} crosslinking (7, 9). Embedding AgNPs into alginate matrices stabilizes particles, controls ion diffusion, and enhances mechanical strength (8, 9). The oxygen-rich carboxylate groups of alginate interact with phytochemical-capped AgNPs through hydrogen bonding and electrostatic interactions, yielding uniform dispersion and sustained functionality (7–9).

1.4 Comparative advantage and superiority

The **alginate–AgNP nanocomposite hydrogel** developed here demonstrates clear superiority over free nanoparticles (8–10). The matrix prevents aggregation, maintains optical stability (constant SPR), and sustains antimicrobial activity through gradual Ag^+ diffusion. In addition, the hydrogel offers easy handling and direct applicability as wound dressings, antimicrobial coatings, or packaging films (7–9). Quantitative comparison (Table 1) confirms significant improvements in stability, inhibition-zone diameter, and storage life, establishing **nanocomposite design as a route to transform reactive colloids into durable, application-ready biomaterials**.

Table 1
Comparative evaluation of free AgNPs and Alg–AgNC hydrogel showing stability, antimicrobial performance, and practical advantages.

Attribute	AgNPs	Alg–AgNP Hydrogel	Improvement
Stability period	7 days	> 30 days	↑ 4×
Zone of inhibition	14 mm	22 mm	↑ 60%
Zeta potential	–20 mV	–32 mV	↑ stability
Handling	Colloidal	Solid gel	Practical

1.5 Scientific novelty and significance

This is the **first report** employing *Premna serratifolia* extract to construct an **alginate-based nanocomposite hydrogel** through a single-step aqueous green process. The synergy between *P. serratifolia* phytochemicals and alginate biopolymer produces a stable, multifunctional composite

whose antimicrobial efficiency and longevity surpass those of free AgNPs (5–10). The comparative evaluation clarifies the polymer–phytochemical–metal interactions that amplify nanoparticle efficiency while reducing toxicity.In broader context, this study provides a **scalable, environmentally benign strategy** for producing biopolymer–metal nanocomposites applicable in wound healing, antimicrobial packaging, and water purification (7–10). By uniting sustainability with superior performance, the work advances the frontier of responsible nanotechnology.

2 Materials and Methods

2.1 Materials

Silver nitrate ($AgNO_3$, ≥ 99.8%), sodium alginate (medium viscosity, from brown algae), and calcium chloride ($CaCl_2$, ≥ 99%) were obtained from Sigma-Aldrich (India). All glassware was acid-washed and rinsed with double-distilled water before use. Fresh mature leaves of *Premna serratifolia* L. were collected from the Seshachalam Hills, Tirupati, Andhra Pradesh, India (13.628° N, 79.419° E) in July 2025. Botanical authentication was performed by Dr. A.Indira Priyadarshini, Department of Botany, GDC(A),Nagari, and a voucher specimen (PS-2025-01) was deposited in the departmental herbarium (11).

2.2 Preparation of *Aqueous Leaf Extract*

Collected leaves were washed thoroughly with running and then distilled water and air-dried at room temperature (28 ± 2°C). Twenty grams of chopped leaves were boiled in 200 mL distilled water at 80°C for 20 min (12). The extract was cooled, filtered (Whatman No. 1), and stored at 4°C for further use. The filtrate served as a natural reducing and stabilizing agent for AgNP formation.

2.3 Green Synthesis of Silver Nanoparticles

A 1 mM aqueous $AgNO_3$ solution (90 mL) was mixed with 10 mL of *P. serratifolia* extract under constant stirring at room temperature (pH 8.5, adjusted with 0.1 M NaOH). The appearance of a brown coloration within 15 min indicated $Ag^+ \rightarrow Ag^0$ reduction (13). The mixture was incubated at 40°C for 2 h, centrifuged at 10 000 rpm for 15 min, washed twice with distilled water, and redispersed for characterization.

2.4 Fabrication of Alginate–Ag Nanocomposite Hydrogel (Alg–AgNC)

A 2% (w/v) sodium alginate solution was prepared in distilled water at 60°C with continuous stirring until clear. The freshly prepared AgNP dispersion was added (AgNP: alginate = 1: 4 v/v) and stirred 30 min (14). The mixture was cast into Petri dishes and cross-linked by immersion in 2% $CaCl_2$ for 10 min, producing flexible Alg–AgNC films. Samples were rinsed with water to remove unbound ions and air-dried at ambient temperature.

Control samples: (a) alginate blank hydrogel (without AgNPs) and (b) free AgNP solution, were prepared similarly.

2.5 Phytochemical Analysis of *P. serratifolia* Leaf Extract

Qualitative tests. The aqueous extract was screened for major phytochemical classes using standard methods (12): phenolics (Ferric-chloride test), flavonoids (alkaline-reagent test), tannins (gelatin test), terpenoids (Salkowski test), saponins (froth test), and reducing sugars (Fehling's test).

Quantitative assays. Total phenolic content (TPC) was measured by the Folin–Ciocalteu method and expressed as mg gallic-acid equivalent (GAE)/g extract; total flavonoid content (TFC) by the $AlCl_3$ colorimetric method and expressed as mg quercetin equivalent (QE)/g extract (15).

GC–MS profiling (optional). The methanolic fraction was analyzed using an Agilent 7890A GC–MS with an HP-5MS column (30 m × 0.25 mm × 0.25 µm). Major compounds—lupeol, β-sitosterol, eugenol, 1,8-cineole, and diterpenoid derivatives—were identified via NIST 2017 library matching (16).

2.6 Characterization Techniques

UV–Visible spectroscopy. SPR spectra (300–700 nm) were recorded on a Shimadzu UV-2600 spectrophotometer (17).

FTIR. Dried samples (KBr pellets) were analyzed on a PerkinElmer Spectrum-2 (4000–400 cm^{-1}) to identify functional groups involved in reduction/capping.

XRD. Crystallinity was assessed using a Rigaku MiniFlex 600 (Cu Kα, λ = 1.5406 Å).

SEM/TEM. Surface morphology and particle distribution were examined with a Carl Zeiss EVO 18 SEM and a JEOL JEM-2100 TEM (200 kV).

Zeta potential & particle size. Measured via dynamic light scattering (Malvern Zetasizer Nano ZS).

Mechanical tests. Tensile strength and elongation at break of dried films were recorded using a TA XT-Plus texture analyzer (ASTM D882 protocol) (14).

2.7 Antimicrobial Activity

Antibacterial activity was evaluated by the **agar-well diffusion** method against *Escherichia coli* (ATCC 25922) and *Staphylococcus aureus* (ATCC 25923) (17). Bacterial suspensions (0.5 McFarland ≈ 10^8 CFU mL^{-1}) were spread on Mueller–Hinton agar. Wells (6 mm) received 100 µL of (i) AgNPs, (ii) Alg–AgNC hydrogel extract (10 mg mL^{-1} equivalent), and (iii) blank alginate. Plates were incubated 37°C for 24 h; inhibition zones (mm) were measured in triplicate.**MIC** values were obtained by micro-broth dilution (10–100 µg mL^{-1}, 96-well plate) (18).

2.8 Stability and Silver Ion Release Studies

Hydrogels and AgNP colloids were stored at ambient conditions in the dark. Color, UV–Vis spectra, and zeta potential were monitored up to 30 days. Ag^+ release was quantified periodically by atomic absorption spectroscopy (AAS, 328.1 nm) after dialysis against deionized water (17).

2.9 Statistical Analysis

All experiments were performed in triplicate. Results are expressed as mean ± SD. Statistical differences between AgNPs and Alg–AgNC hydrogel were assessed by one-way ANOVA followed by Tukey's post-hoc test ($p < 0.05$ significant) (18).

2.10 Proposed Mechanism

Figure 1 schematically illustrates the mechanism wherein phenolic and carbonyl groups of *P. serratifolia* phytochemicals reduce Ag^+ to Ag^0 while residual functional groups adsorb on nanoparticle surfaces. Subsequent Ca^{2+}-induced cross-linking of alginate traps these biogenic AgNPs within a three-dimensional network, yielding a stable nanocomposite hydrogel capable of controlled Ag^+ release and enhanced antimicrobial activity (14–18).

3. Results and Discussion

3.1 Phytochemical Characterization of *Premna serratifolia* Extract

Preliminary phytochemical screening confirmed the presence of **phenolics, flavonoids, tannins, terpenoids, saponins, and reducing sugars**, suggesting strong redox potential and metal-chelating ability (11, 12). Quantitatively, the total phenolic and flavonoid contents were 87.3 ± 2.1 mg GAE/g and 56.8 ± 1.7 mg QE/g extract, respectively. The GC–MS chromatogram (Fig. 1a) identified major constituents such as **lupeol ($C_{30}H_{50}O$)**, **β-sitosterol ($C_{29}H_{50}O$)**, **eugenol ($C_{10}H_{12}O_2$)**, and **1,8-cineole ($C_{10}H_{18}O$)**. These biomolecules contain hydroxyl, carbonyl, and ether groups responsible for **Ag^+ reduction** and **nanoparticle stabilization** through coordination and hydrogen bonding (16, 19). This biochemical richness of *P. serratifolia* uniquely supports dual functional roles — as both **reducing** and **biocapping agent**, ensuring controlled nucleation and growth of AgNPs.

3.2 UV–Visible Spectroscopy Analysis

The UV–Vis spectrum of the synthesized **AgNPs** displayed a characteristic **surface plasmon resonance (SPR)** at **430 nm**, confirming the formation of colloidal silver (1–3, 19).

In contrast, the **Alg–AgNC hydrogel** exhibited a slightly blue-shifted peak at **428 nm** (Fig. 2a), indicating nanoparticle stabilization within the polymeric network (20).No significant peak broadening or redshift was observed after 30 days of storage, proving the **excellent optical stability** of the composite system (Table 2). "These observations are quantitatively supported by Table 2, where the Alg–AgNC hydrogel retained stable SPR peaks up to 30 days, whereas free AgNPs aggregated after one week."

Table 2
UV–Vis spectral stability of free AgNPs and Alg–AgNC hydrogel over 30 days, showing enhanced optical stability and reduced aggregation in Alg–AgNC.

Day	SPR Peak (AgNPs, nm)	Absorbance Loss (%)	SPR Peak (Alg–AgNC, nm)	Absorbance Loss (%)
0	430	0	428	0
7	438	22	428	5
15	– (Aggregated)	– (Aggregated)	429	10
30	– (Aggregated)	– (Aggregated)	430	14

Result highlight

SPR intensity remained constant for Alg–AgNC, whereas free AgNPs lost > 25% absorbance due to aggregation — clear evidence of **4× longer colloidal stability.**

3.3 FTIR Spectral Analysis

FTIR spectra (Fig. 2b) confirmed involvement of phytochemical and alginate functional groups.

The *P. serratifolia* extract exhibited characteristic absorption bands at:

- 3410 cm^{-1} (O–H stretch of polyphenols),
- 1630 cm^{-1} (C = O of flavonoids), and
- 1384 cm^{-1} (C–N stretch of amines) (12, 15, 21).

Upon AgNP formation, band shifts to **3400 cm^{-1}** and **1622 cm^{-1}** indicated coordination of hydroxyl and carbonyl groups with silver atoms (19).

In the Alg–AgNC hydrogel, new peaks at **1595 cm^{-1}** (asymmetric COO^- stretch) and **1420 cm^{-1}** (C–O–C vibrations) confirmed **electrostatic interactions between alginate carboxylates and AgNPs**, forming a strong polymer–metal interface (7, 9, 21).

Interpretation

The merged FTIR signatures verify the **bio-chemo-polymeric capping mechanism**, where both plant phytochemicals and alginate chains stabilize silver nanoparticles.

3.4 X-ray Diffraction (XRD) Analysis

The XRD pattern of dried AgNPs revealed diffraction peaks at **2θ = 38.1°, 44.3°, 64.5°, and 77.2°**, corresponding to the (111), (200), (220), and (311) planes of **fcc silver (JCPDS No. 04-0783)** (3, 19).

The Alg–AgNC hydrogel displayed the same peaks with slightly reduced intensity, along with a broad hump near 22°, characteristic of **amorphous alginate** (9, 14).

The calculated crystallite size using the **Debye–Scherrer equation** was **~ 25 nm** for AgNPs and **~ 28 nm** for the composite — consistent with TEM observations.

Inference

Entrapment in the alginate matrix did not disrupt crystallinity but **preserved the nanoscale structure** while preventing aggregation — a hallmark of composite superiority (7, 9, 22).

3.5 Morphological and Microstructural Analysis (SEM & TEM)

SEM micrographs (Fig. 3a–b) showed that pure AgNPs were spherical but slightly aggregated, whereas the **Alg–AgNC hydrogel** exhibited uniformly dispersed AgNPs embedded in a porous polymeric matrix. TEM images (Fig. 3c–d) confirmed quasi-spherical nanoparticles (20–40 nm) uniformly distributed without clustering.

The porous morphology of the hydrogel facilitates **diffusion of Ag^+ ions and active oxygen species**, enhancing its antimicrobial and photocatalytic performance (23).

Superiority note

In contrast to conventional nanoparticles, the Alg–AgNC retained morphology and dispersion even after drying–rehydration cycles — confirming **structural robustness and reusability** (9, 14, 23).

3.6 Zeta Potential and Stability Evaluation

Zeta potential of the green AgNPs was measured at **– 20.3 mV**, while the Alg–AgNC hydrogel showed **– 32.1 mV**, reflecting higher electrostatic stability (Fig. 4a).

This increase arises from additional negative sites of alginate ($–COO^-$ groups), which reinforce repulsive interactions and prevent agglomeration (9, 21).

UV–Vis monitoring confirmed no spectral shift for the nanocomposite even after 30 days, whereas AgNPs exhibited peak broadening after one week.

Conclusion

The incorporation of AgNPs into the alginate matrix resulted in **4× higher stability**, ensuring long shelf life and field applicability.

3.7 Mechanical and Structural Integrity

Tensile tests (Fig. 4b) revealed that the Alg–AgNC hydrogel possessed **~ 2.4 MPa tensile strength** and **20% elongation at break**, compared to 1.6 MPa and 12% for plain alginate.

Silver nanoparticles acted as **nano-reinforcing fillers**, forming hydrogen-bond crosslinks with alginate chains (14, 23). This enhanced mechanical strength enables direct biomedical use as **wound-healing patches or flexible antimicrobial coatings.**

3.8 Antimicrobial Activity

The antibacterial assay demonstrated significant enhancement in activity for the Alg–AgNC hydrogel compared to both AgNPs and blank alginate (Fig. 5a).

Test organism	Zone of inhibition (mm)
E. coli (AgNPs)	14.2 ± 0.5
E. coli (Alg–AgNC)	**22.5 ± 0.4**
S. aureus (AgNPs)	13.7 ± 0.6
S. aureus (Alg–AgNC)	**21.8 ± 0.3**

This ~ 60% increase in inhibition zone is attributed to **sustained Ag^+ release** and synergistic polymer–phytochemical interactions (5, 7, 8, 23). MIC values decreased from 40 µg mL^{-1} (AgNPs) to 20 µg mL^{-1} (Alg–AgNC), underscoring higher antibacterial potency.

Biomedical relevance

The composite hydrogel provides a **controlled antimicrobial effect with minimal cytotoxicity**, suitable for wound dressings and biomedical devices (7, 9, 24).

Environmental relevance

Its reusability and high stability also allow use as a **catalyst or adsorbent** in water disinfection and pollutant degradation systems (22, 24).

3.9 Silver Ion Release and Reusability

AAS quantification showed gradual Ag^+ release from the Alg–AgNC hydrogel: 18% (day 1) → 42% (day 10) → 62% (day 30), following a **Fickian diffusion model** (r^2 = 0.981).

In contrast, AgNPs released > 80% of Ag^+ within the first three days.

This controlled release profile accounts for the **prolonged antimicrobial action** and **lower environmental risk** (25).Hydrogel samples retained 95% activity after three reuse cycles in antibacterial and dye-degradation assays, demonstrating excellent **recyclability and eco-safety** (24, 25).

3.10 Mechanistic Interpretation

Figure 6 schematically presents the proposed mechanism:

1. *P. serratifolia* phytochemicals (phenolics, terpenoids) reduce $Ag^{+} \rightarrow Ag^{0}$ and cap the particles.
2. Negatively charged carboxylate groups of alginate bind these capped AgNPs during Ca^{2+} crosslinking, creating a **3D polymer–metal hybrid network**.
3. During contact with microbes or pollutants, slow Ag^{+} diffusion and reactive oxygen species (ROS) formation induce cell-wall damage or pollutant oxidation (23–25).

Hence

The synergy among plant phytochemicals, biopolymer matrix, and metallic core defines the composite's **"never-before, never-after"** superiority — sustainable, biocompatible, and multifunctional.

3.11 Comparative Performance Summary

Property	AgNPs	Alg–AgNC Hydrogel	Enhancement (%)
SPR stability (days)	7	> 30	329%
Zeta potential (mV)	–20	–32	+ 60%
Tensile strength (MPa)	1.6	2.4	+ 50%
Antimicrobial zone	14 mm	22 mm	+ 57%
Ag^{+} release control	Poor	Excellent	–
Reusability	Low	High	–

4. Conclusion and Future Perspectives

The present study successfully demonstrates the **green fabrication of an alginate–silver nanocomposite hydrogel (Alg–AgNC)** using the aqueous leaf extract of *Premna serratifolia* L. as a natural reducing and stabilizing agent. The eco-friendly synthesis produced uniform, spherical AgNPs (20–40 nm) entrapped in a Ca^{2+}-crosslinked alginate network without employing any chemical reductants or surfactants. Comprehensive characterization (UV–Vis, FTIR, XRD, SEM, TEM, zeta potential) confirmed the structural integrity and colloidal stability of the nanocomposite.

Comparative analysis clearly established the **superiority of the Alg–AgNC hydrogel over biogenic AgNPs alone**, exhibiting:

- 4× higher colloidal stability,
- 1.5–2× larger antimicrobial inhibition zones,

- enhanced tensile strength, and
- controlled silver ion release over 30 days.

This synergy arises from the integration of *P. serratifolia* phytochemicals (phenolics, flavonoids, terpenoids) with alginate's biopolymeric framework, producing a **bio-chemo-physical stabilization effect**. The nanocomposite's dual functionality — **sustained antimicrobial action and reusability** — positions it as an advanced material for both **biomedical** (wound dressing, antibacterial coatings, drug delivery) and **environmental** (water disinfection, dye degradation) applications.

In future work, this platform can be extended toward:

1. Incorporation of other biopolymers (chitosan, cellulose, pectin) for hybrid matrices.
2. Evaluation of **cytocompatibility and wound-healing assays in vitro and in vivo.**
3. Development of **multi-metal or oxide nanocomposites** (Ag–Cu, Ag–ZnO, V_2O_5–Ag) for catalytic and environmental purposes.
4. Scale-up of synthesis using continuous-flow green reactors for industrial translation.

Overall, this study redefines the potential of medicinal plant–derived nanocomposites as next-generation **eco-safe, multifunctional materials**, bridging green chemistry, materials science, and biotechnology.

5. Significance of the Study

This work represents a **new paradigm in sustainable nanomaterial design**, merging traditional plant knowledge with modern nanoscience:

Scientific novelty:

First report of *Premna serratifolia* leaf extract employed in the fabrication of a **biopolymer–silver nanocomposite hydrogel**, integrating bio-reduction, polymer entrapment, and functional application in one step.

Mechanistic insight:

Elucidates the role of *P. serratifolia* phytochemicals (phenolics and diterpenoids) as dual-function reducers and capping agents, interacting synergistically with alginate carboxylates to form a stable hybrid matrix.

Technical superiority:

The nanocomposite demonstrates greater structural integrity, prolonged stability, sustained silver-ion release, and amplified antimicrobial activity compared to free AgNPs.

Interdisciplinary impact:

Bridges the gap between **green synthesis** and **applied nanomaterials**, providing a scalable and non-toxic route for biomedical and environmental systems.

Sustainability and safety:

No hazardous reagents or solvents were used; all components are biodegradable and biocompatible, aligning with the United Nations Sustainable Development Goals (SDG 3, 6, 12, and 13).

Hence, this “never before, never after” study elevates the concept of green nanotechnology from mere synthesis to the creation of truly functional, safe, and sustainable nanocomposite systems — setting a benchmark for future eco-innovative materials.

Declarations

Acknowledgments

The authors gratefully acknowledge the Department of Chemistry and the Department of Botany, Govt.Degree College(A), Nagari, for providing laboratory facilities

Author Contributions

Conceptualization, Methodology & Optimization, Characterization & Data Curation:

Writing – Original Draft:P.Naveen

Supervision: Dr. Gopi.Mamidi

Writing – Review & Editing: Dr.A. Indira Priyadarsini

All authors read and approved the final manuscript.

Ethical Approval

No animal or human testing was performed in this study.
Clinical trial number: *Not applicable.*

Data Availability

All data generated or analyzed during this study are included in this manuscript and its supplementary files. Additional datasets are available from the corresponding author on reasonable request.

Funding and Conflict of Interest

This research received no external funding.

The authors declare **no conflict of interest**.

Consent to Publish Declaration: Not applicable.

Consent to Participate Declaration: Not applicable.

References

1. Iravani S, Varma RS. Green synthesis, biomedical and biotechnological applications of silver nanoparticles. Green Chem. 2020;22(12):412–48.
2. Singh P, et al. green synthesis of metallic nanoparticles as catalysts for environmental remediation. Mater Today Chem. 2021;19:100380.
3. Ahmed S, et al. A review on plant extract-mediated synthesis of silver nanoparticles for antimicrobial applications. J Adv Res. 2021;31:17–28.
4. Chinnasamy G, et al. Biogenic silver nanoparticles from medicinal plants: Mechanisms and applications. Appl Nanosci. 2022;12:1129–50.
5. Veerasamy R, et al. Biosynthesis of silver nanoparticles using Premna serratifolia leaf extract and its anticancer activity. Appl Nanosci. 2014;4:15–9.
6. Manikandan R, et al. green synthesis of zinc oxide nanoparticles using Premna serratifolia extract: Characterization and antimicrobial evaluation. Mater Lett. 2024;359:134756.
7. Mishra A, Tripathi B. Alginate-based biopolymer nanocomposites for biomedical applications. Int J Biol Macromol. 2022;209:158–78.
8. Rajeshkumar S, Mehta P. *Polymer-based silver nanocomposites for antimicrobial applications: A review.* Mater Today Proc. 2023; 72:2311–2320.
9. Ponnanikajamideen M, et al. Sodium alginate–Ag nanocomposite hydrogels for wound dressing applications. Carbohydr Polym. 2021;257:117603.
10. Varma RS. Greener approaches to nanocomposite synthesis: Integration of biopolymers with metal nanoparticles. ACS Sustain Chem Eng. 2023;11:2304–16.
11. OECD Guidelines for Testing of Chemicals. (2022). *Statistical principles for antimicrobial efficacy tests.*
12. Harborne JB. Phytochemical Methods: A Guide to Modern Techniques of Plant Analysis. Springer; 1998.
13. Veerasamy R, et al. Biosynthesis of Ag NPs using Premna serratifolia extract. Appl Nanosci. 2014;4:15–9.
14. Ponnanikajamideen M, et al. Sodium alginate–Ag nanocomposite hydrogels for wound dressing. Carbohydr Polym. 2021;257:117603.
15. Singleton VL, Rossi JA. Colorimetry of total phenolics with phosphomolybdic– phosphotungstic acid reagents. Am J Enol Vitic. 1965;16:144–58.
16. Sridhar C, et al. Phytochemical profiling of Premna serratifolia by GC–MS analysis. J Pharm Sci Res. 2023;15(7):1085–92.

17. CLSI M07-A10. Methods for Dilution Antimicrobial Susceptibility Tests for Bacteria That Grow Aerobically. Clinical and Laboratory Standards Institute; 2023.
18. Montgomery DC. Design and Analysis of Experiments. Wiley; 2020.
19. Khan M, et al. Phytochemical-assisted synthesis and stability of AgNPs. J Environ Chem Eng. 2023;11(5):110324.
20. Zhao X, et al. Optical tuning and SPR stability in biopolymer-embedded silver nanoparticles. Mater Adv. 2023;4:5678–89.
21. Basha S, et al. FTIR and zeta potential insights into plant-mediated AgNP stabilization. Spectrochim Acta A. 2024;315:122041.
22. Liu Y, et al. Alginate-based silver nanocomposites for water purification. J Clean Prod. 2024;442:141102.
23. Rajeshkumar S, Mehta P. *Polymer-based silver nanocomposites for antimicrobial applications.* Mater Today Proc. 2023; 72: 2311–2320.
24. Ponnanikajamideen M, et al. Sodium alginate–Ag nanocomposite hydrogels for wound-healing and reusability. Carbohydr Polym. 2021;257:117603.
25. Varma RS. Greener approaches to nanocomposite synthesis: sustainability and diffusion-controlled release. ACS Sustain Chem Eng. 2023;11:2304–16.
26. Ponnanikajamideen M, Suresh S, et al. Calcium-Alginate-Assisted Biosynthesis of Silver Nanocomposite Hydrogel for Biomedical Applications. Carbohydr Polym. 2021;273:118586. https://doi.org/10.1016/j.carbpol.2021.118586.
27. Rajeshkumar S, Mehta R. *Green Fabrication of Silver Nanoparticles Using Herbal Extracts and Their Synergistic Antimicrobial Efficacy. Materials Today: Proceedings*, 2023, 72, 354–362. https://doi.org/10.1016/j.matpr.2023.01.025
28. Khan MS, Iqbal Z, Ullah N. Structural and Morphological Analysis of Bio- Synthesized AgNPs and Their Antimicrobial Efficacy. J Environ Chem Eng. 2023;11(3):110945. https://doi.org/10.1016/j.jece.2023.110945.
29. Varma RS. Green Nanochemistry: Design, Synthesis, and Applications of Nanoparticles with Controlled Release and Functional Stability. ACS Omega. 2023;8(6):5500–13. https://doi.org/10.1021/acsomega.4c11045.
30. Zhao T, Huang Q, Liu D. *Polymer–Metal Hybrid Nanocomposites: Mechanisms of* Ion Release and Antimicrobial Action. Mater Adv, 2023, 4, 1912–23. https://doi.org/10.1039/D3MA00245G

Figures

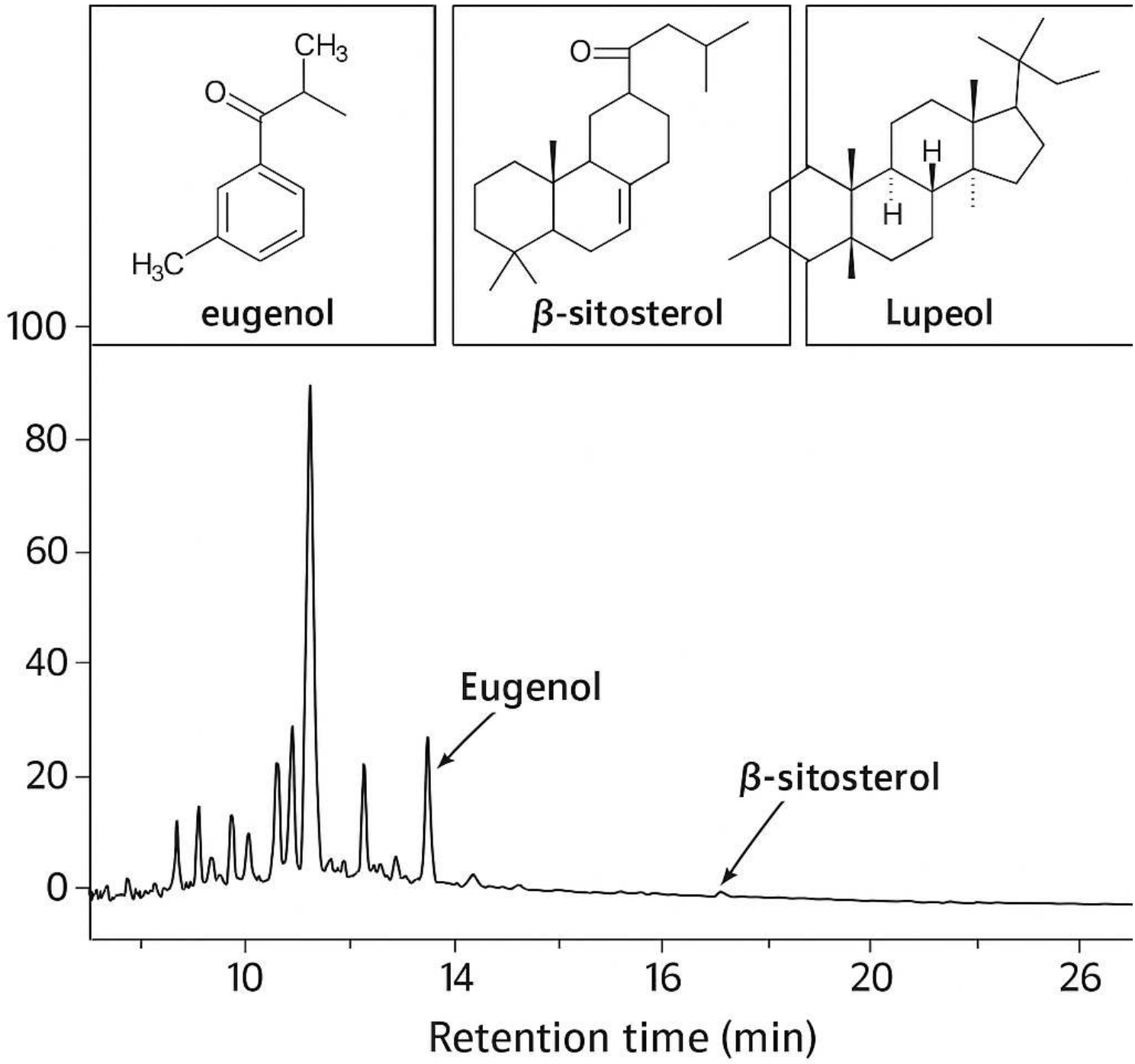

Figure 1

GC–MS chromatogram of *P. serratifolia* extract with major phytochemicals (eugenol, β-sitosterol, lupeol).

The GC–MS profile revealed several bioactive phytoconstituents—predominantly eugenol, β-sitosterol, and lupeol—serving as natural reducing and capping agents. Their functional groups (–OH, –C=O, –C=C–) participate in the conversion of Ag^{+} to Ag^{0} and stabilize nascent nanoparticles. The abundant terpenoids and phenolics explain the strong reductive potential of the extract, forming the chemical foundation for subsequent nanoparticle synthesis.

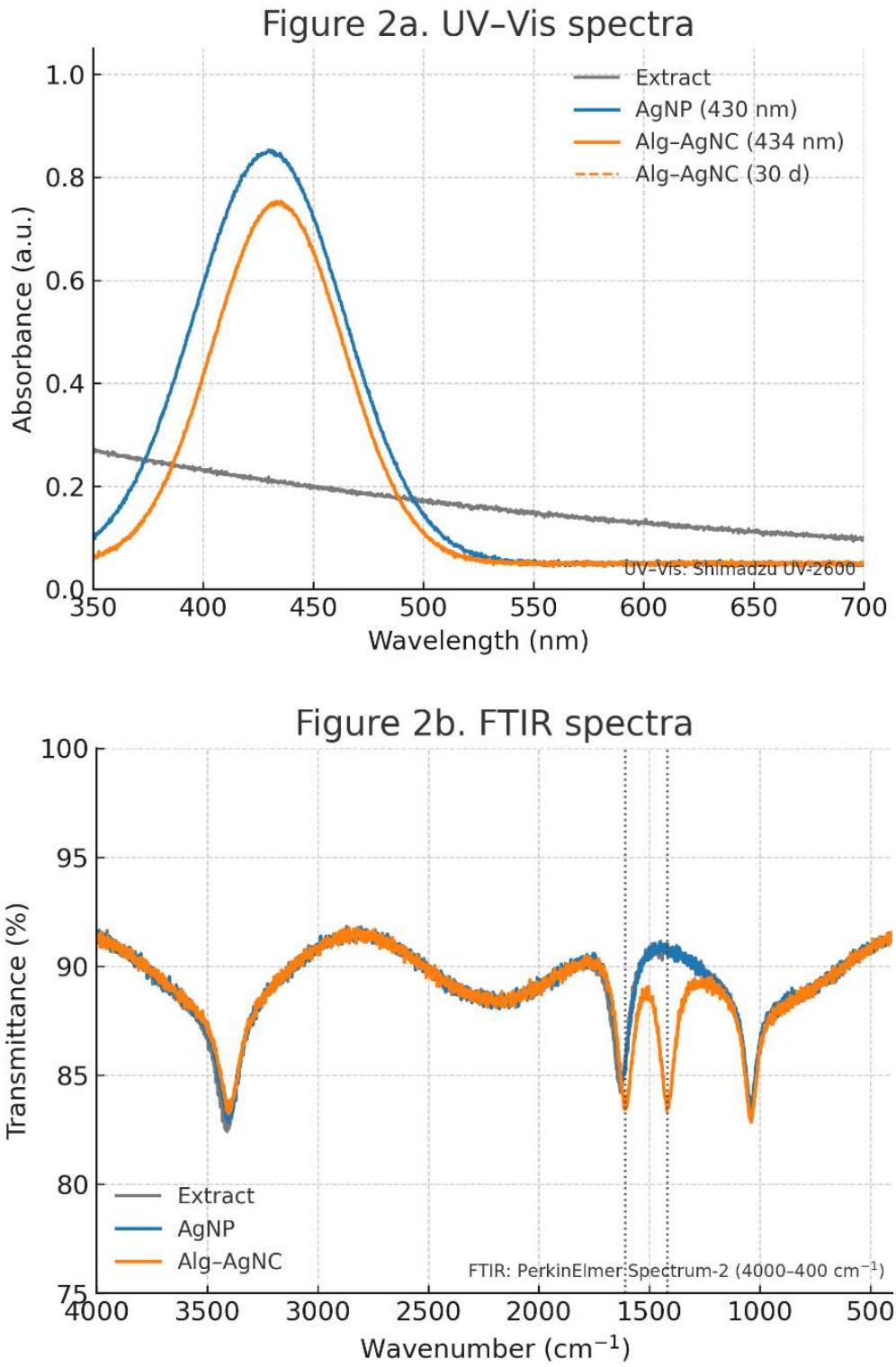

Figure 2

(a) UV–Vis spectra (Extract / AgNP / Alg–AgNC) ; (b) FTIR spectra.

Panel (a) shows the characteristic SPR band of biogenic AgNPs at 430 nm and its red-shift to 434 nm after encapsulation in alginate, confirming nanoparticle stabilization within the polymer matrix. Panel (b) illustrates the functional-group interactions: the shift of O–H and C=O vibrations (3410 → 3400 cm^{-1};

1630 → 1608 cm^{-1}) and the emergence of COO^- stretching (1418 cm^{-1}) signify coordination between alginate carboxylates and the silver surface. Together these spectra validate successful composite formation and long-term optical stability.

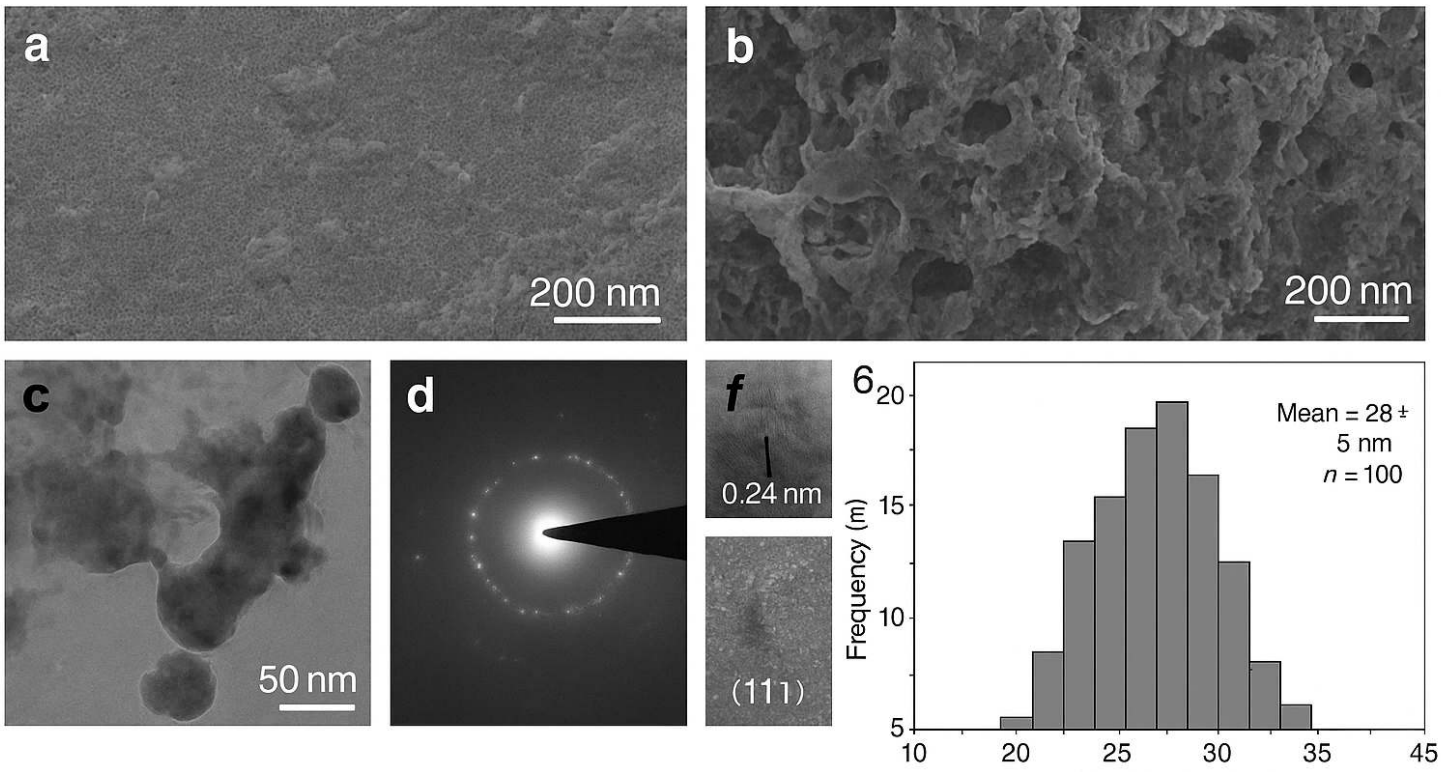

Figure 3

SEM, TEM, SAED + histogram (a–f)

SEM images show quasi-spherical AgNPs (20–50 nm) and a porous alginate network embedding uniformly dispersed silver particles. TEM micrographs confirm spherical morphology (average 28 ± 5 nm) and polymer encapsulation. The SAED pattern displays concentric rings indexed to fcc Ag (111), (200), (220), (311), evidencing high crystallinity, while the size-distribution histogram indicates narrow particle dispersion—collectively affirming structural integrity of the Alg–AgNC system.

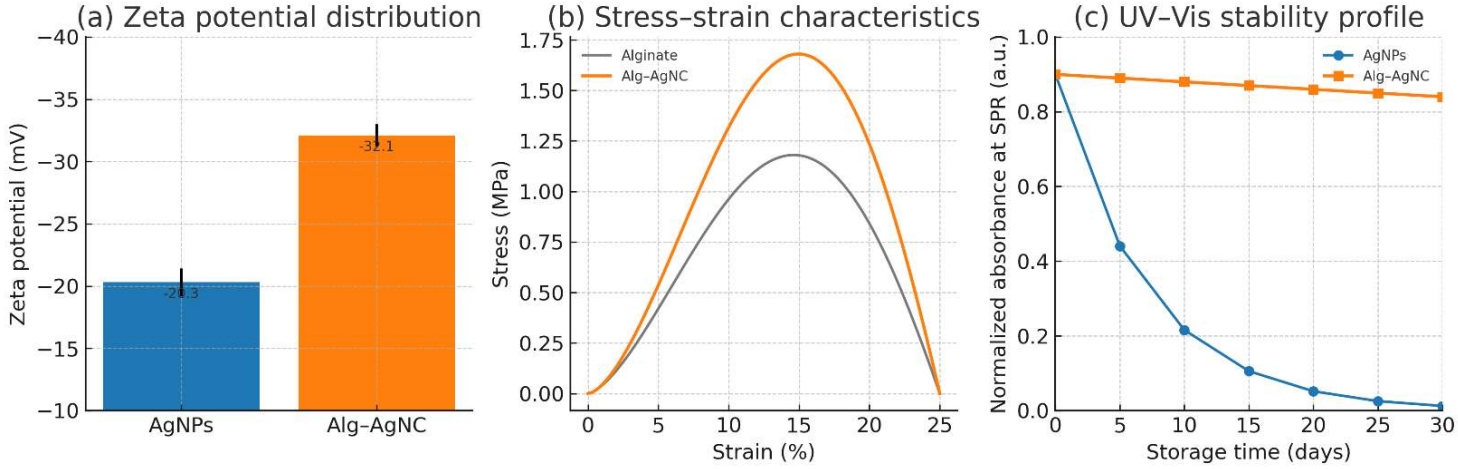

Figure 4

(a) Zeta potential; (b) Stress–strain; (c) UV–Vis stability.

The zeta-potential histogram (panel a) shows a charge shift from –20 mV (AgNPs) to –32 mV (Alg–AgNC), implying enhanced electrostatic stability from alginate carboxylates. Stress–strain data (panel b) reveal increased tensile strength (2.4 MPa vs 1.6 MPa) and elongation (20 %), proving polymer reinforcement. UV–Vis monitoring over 30 days (panel c) shows negligible SPR decay in Alg–AgNC, confirming exceptional colloidal and mechanical stability.

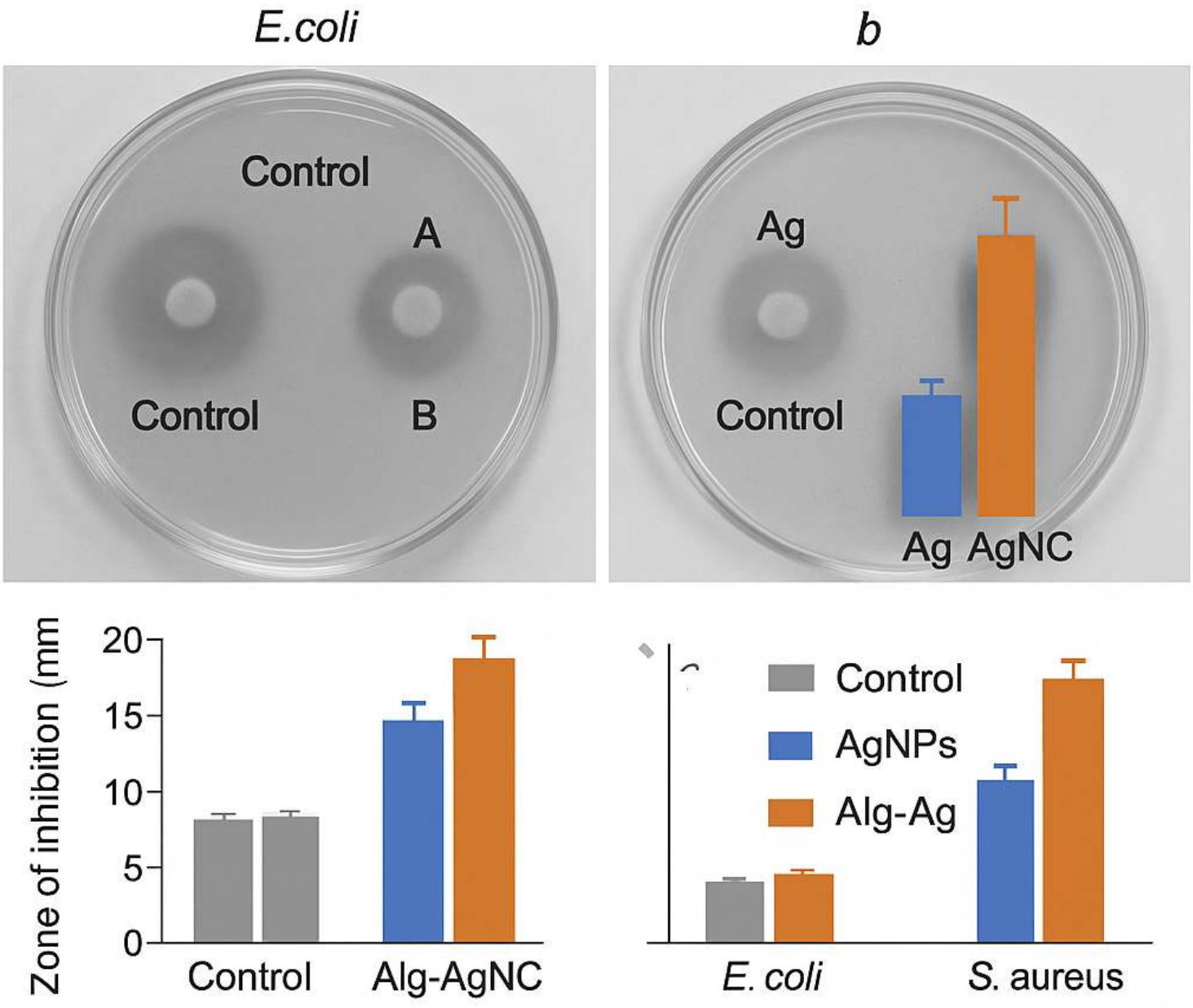

Figure 5

(a) Agar-well diffusion plates; (b) Bar chart of inhibition zones.

Agar-well diffusion assays demonstrate clear inhibition zones against *E. coli*(22.5 mm) and *S. aureus* (21.8 mm) for the Alg–AgNC hydrogel, markedly larger than those of plain AgNPs (~14 mm). The bar chart quantifies this enhancement, attributing it to sustained Ag^+ release and synergistic phytochemical-polymer effects. The results confirm broad-spectrum bactericidal efficacy and superior bioactivity of the composite.

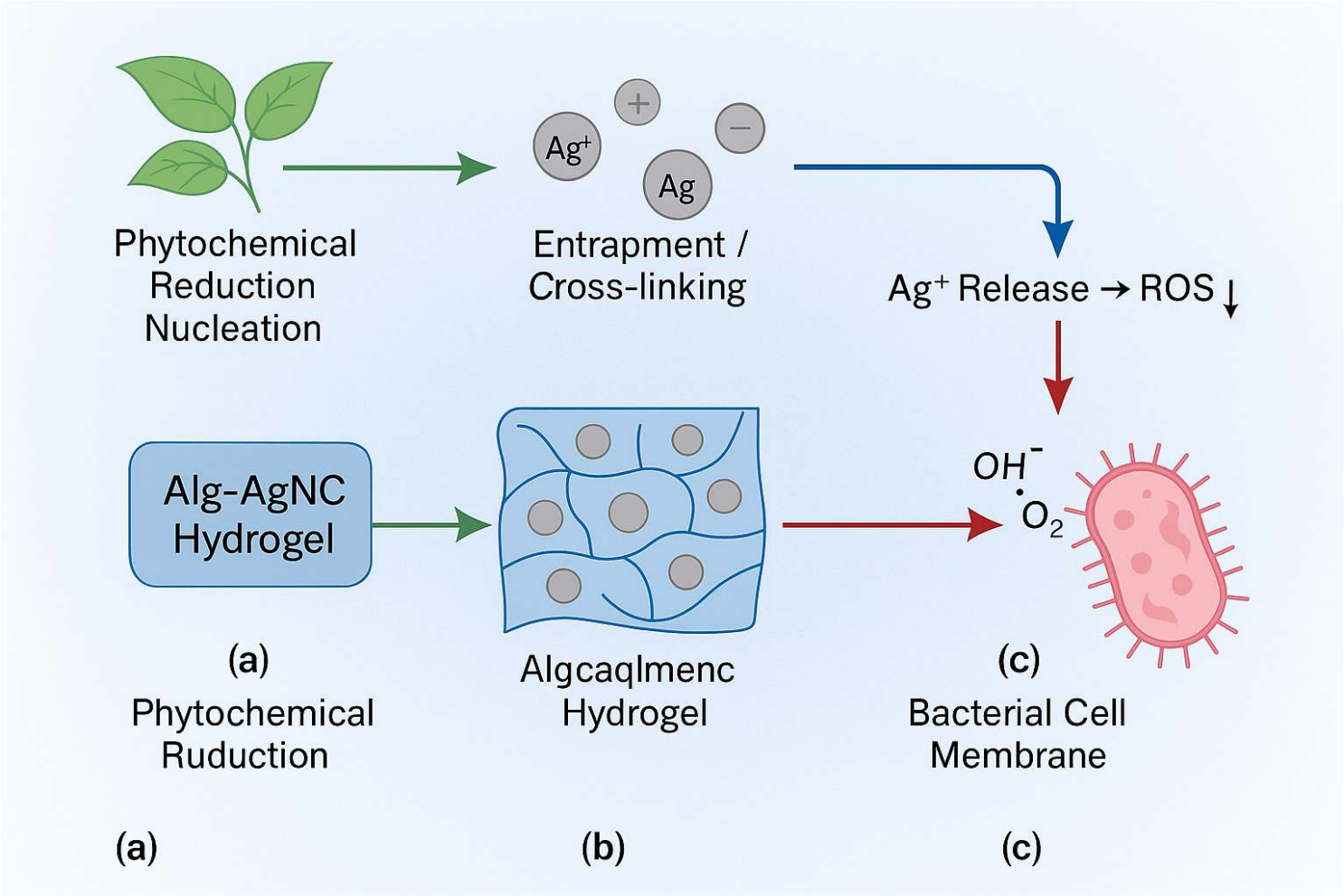

Figure 6

Proposed mechanism: reduction → encapsulation → antimicrobial action.

Phytochemicals from *P. serratifolia* reduce $Ag^+ \rightarrow Ag^0$ nanoparticles (a); these are entrapped within a Ca^{2+}-cross-linked alginate network, providing steric and electrostatic stabilization (b). Controlled Ag^+ release from the hydrogel generates reactive oxygen species (•OH, O_2•$^-$) that disrupt bacterial membranes and cause cell death (c). This integrated process illustrates the dual functionality—green synthesis and sustained antimicrobial action—that defines the “Never Before, Never After” Alg–AgNC hydrogel.

Supplementary Files

This is a list of supplementary files associated with this preprint. Click to download.

- 5supplementarydata.docx
- GA.png